

Split magnetization steps in $\text{Cd}_{1-x}\text{Mn}_x\text{Se}$: Inequivalent nearest neighbors and the Dzyaloshinski-Moriya interaction

V. Bindilatti,* T. Q. Vu, and Y. Shapira

Department of Physics and Astronomy, Tufts University, Medford, Massachusetts 02155

C. C. Agosta and E. J. McNiff, Jr.

Francis Bitter National Magnet Laboratory, Massachusetts Institute of Technology, Cambridge, Massachusetts 02139

R. Kershaw, K. Dwight, and A. Wold

Department of Chemistry, Brown University, Providence, Rhode Island 02912

(Received 30 August 1991)

In the wurtzite structure the twelve nearest-neighbor (NN) cations surrounding a given cation belong to two groups: six "in" NN's that are in the same c plane, and six "out" NN's that are out of the c plane. These two groups are inequivalent, by symmetry, and the NN exchange constants J_1^{in} and J_1^{out} are unequal. The difference $\Delta J_1 \equiv J_1^{\text{in}} - J_1^{\text{out}}$ gives rise to a splitting of the magnetization steps (MST's) associated with pairs of NN magnetic ions. Each MST splits into two "half-steps," one due to in pairs, and the other due to out pairs. The average J_1 , and the absolute value of the difference ΔJ_1 between the two J_1 's, are obtained from the fields at the half steps. Analysis of the line shape of the split MST's yields the sign of ΔJ_1 and an estimate for the Dzyaloshinski-Moriya interaction constant D . These procedures were implemented for $\text{Cd}_{1-x}\text{Mn}_x\text{Se}$ with $x = 0.010$ and 0.025 . The first two MST's were observed at 0.5 – 0.6 K in experiments that used magnetic fields up to 30 T. At these temperatures only the splitting of the second MST was resolved. The splitting of the first MST was observed at 0.08 K, in experiments up to 20 T. The average NN exchange constant $\bar{J}_1 \equiv \frac{1}{2}(J_1^{\text{in}} + J_1^{\text{out}})$ is $\bar{J}_1/k_B = -7.55 \pm 0.1$ K, and the magnitude of the difference is $|\Delta J_1|/\bar{J}_1 = 0.15 \pm 0.01$. The latter value is in good agreement with a theoretical estimate by Larson. Line-shape analysis indicates that J_1^{in} is larger in magnitude than J_1^{out} , as predicted by Larson, and it places D in the range $0.10 < D/k_B < 0.24$ K. An alternative analysis of the line shape of the second MST gives the estimate $D/k_B \cong 0.21$ K. These results for D compare well with the value $D/k_B = 0.16$ K predicted by Larson and Ehrenreich.

I. INTRODUCTION

Dilute magnetic semiconductors (DMS) are compound semiconductors in which some of the cations are magnetic.^{1–4} The most extensively studied DMS are II-VI semiconductors containing Mn^{2+} . These materials have either the zinc-blende or the wurtzite structure. In the zinc-blende case the cations form an fcc (face-centered cubic) lattice. In the ideal wurtzite structure they form an hcp (hexagonal-close-packed) structure. In either case, any cation chosen as the "central" cation is surrounded by 12 nearest-neighbor (NN) cations.

In the zinc-blende structure all 12 NN's are equivalent by symmetry. In the wurtzite structure, on the other hand, there are two distinct groups of NN's: (a) six "in-plane" NN's in the same c plane as the central cation, and (b) six "out-of-plane" NN's (three NN's above, and three below the c plane). The two types of NN's are shown in Fig. 1. Even in the ideal wurtzite structure, when $c/a = (8/3)^{1/2} = 1.633$ and all NN's are equidistant from the central cation, the crystal symmetry implies that the two groups are inequivalent. In an actual wurtzite structure there is also a small difference between the distances from the central cation. For CdSe, $c/a = 1.632$, and the difference between the distances is only 0.04% .

Hereafter, the in-plane and out-of-plane NN's will be called the IN and OUT NN's, respectively.

The exchange interactions between the Mn^{2+} ions in II-VI DMS are antiferromagnetic, and are mainly due to superexchange.⁵ The strongest interaction is between NN's. Typically, the NN exchange constant $J_{\text{NN}} \equiv J_1$ is $J_1/k_B \sim -10$ K (Ref. 6), where k_B is the Boltzmann constant. The exchange constant J_2 for next-nearest neighbors (NNN's) is an order of magnitude smaller. Interactions with more distance neighbors are still smaller.⁵

In early works, all NN's in the wurtzite structure were treated as equivalent. Recently, however, it became clear that the NN exchange constant J_1^{in} for the IN NN's differs from J_1^{out} for the OUT NN's. The first suggestion of this difference came from Raman scattering involving NN Mn^{2+} pairs in $\text{Cd}_{1-x}\text{Mn}_x\text{S}$ (Ref. 7). Subsequently the magnitude (but not the sign) of the difference $\Delta J_1 \equiv J_1^{\text{in}} - J_1^{\text{out}}$ in the same system was determined from the splitting of the magnetization steps (MST's).⁸ The difference ΔJ_1 turned out to be fairly small, $|\Delta J_1/\bar{J}_1| \cong 0.13$, where $\bar{J}_1 = \frac{1}{2}(J_1^{\text{in}} + J_1^{\text{out}})$ is the average value of J_1 . The fact that the difference is small is not surprising: In a real-space picture the dominant superexchange path for NN's is through the intervening anion. This dominant path is the same for all NN's in the ideal

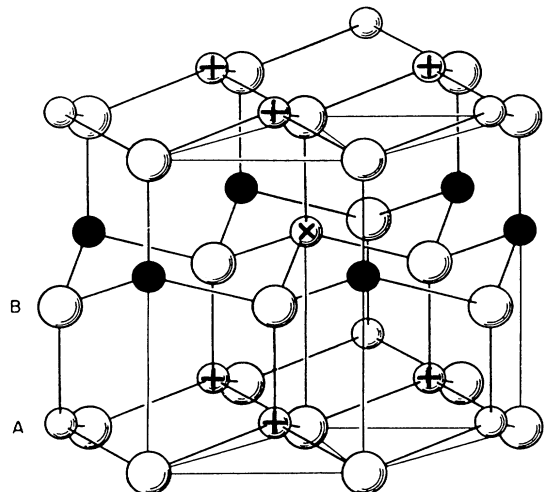


FIG. 1. The wurtzite crystal structure. The small spheres (A) are the cations, and the large spheres (B) are the anions. Any "central cation" (marked by X) is surrounded by six in-plane nearest-neighbor cations (solid spheres), and six out-of-plane nearest-neighbor cations (marked by +).

wurtzite structure. The difference ΔJ_1 is therefore due to other exchange paths.⁸ A recent calculation by Larson⁹ gave $\Delta J_1/J_1 \cong 0.16$. The positive sign implies that J_1^{in} is larger in magnitude than J_1^{out} . These theoretical results for the magnitude and sign of $\Delta J_1/\bar{J}_1$ were obtained for $\text{Zn}_{1-x}\text{Mn}_x\text{Se}$ (when it has the wurtzite structure), but they are expected to hold also for other wurtzite DMS.

In the present work both the magnitude and the sign of ΔJ_1 in $\text{Cd}_{1-x}\text{Mn}_x\text{Se}$ (wurtzite) were obtained from an analysis of the splitting of the first and second magnetization steps.¹⁰ The analysis also yielded estimates of the Dzyaloshinski-Moriya interaction constant D for NN's. These estimates are reasonably close to the theoretical prediction of Larson and Ehrenreich.¹¹

II. THEORETICAL BACKGROUND

Accurate values for J_1 can be obtained from studies of the magnetization steps (MST's). The theory of the MST's has been reviewed recently.⁶ A summary of pertinent theoretical results, with new relevant additions, is given below.

A. MST's when all NN's are equivalent

In this section, we assume that all NN's are equivalent. The physics of the MST's is then reviewed starting from the simple NN cluster model. More general models for equivalent NN's are reviewed later. Theoretical results for materials with inequivalent NN's are discussed in Sec. II B.

1. NN cluster model

In the NN cluster model the only magnetic interaction between magnetic ions is the exchange interaction be-

tween NN's. All magnetic ions are then divided into clusters, the smallest of which are "singles" (with no NN's) and NN pairs. For the samples studied in the present work the great majority of spins are in these two types of clusters (99% for $x=0.01$, and 93% for $x=0.025$)

When a magnetic field H is applied at a low temperature, the spins of the singles align readily. Once this alignment is completed, the magnetization M reaches a plateau, at a value $M=M_s$. The magnetization steps usually appear at higher fields, i.e., they rise above the plateau $M=M_s$. These MST's are due to NN pairs.

The theory of the MST starts from the Hamiltonian for a NN pair,

$$\mathcal{H} = -2J_1 \mathbf{S}_1 \cdot \mathbf{S}_2 + g\mu_B H(S_{1z} + S_{2z}), \quad (1)$$

where \mathbf{S}_1 and \mathbf{S}_2 are individual spins of the Mn^{2+} ions in the pair, g is the g factor, μ_B is the Bohr magneton, and H is taken to be along the z axis. For Mn^{2+} ions the g factor is very close to 2.00. The eigenstates $|S_T m\rangle$ of the Hamiltonian (1) are characterized by the magnitude S_T of the total spin of the pair, and the component m of \mathbf{S}_T along H . The energies are

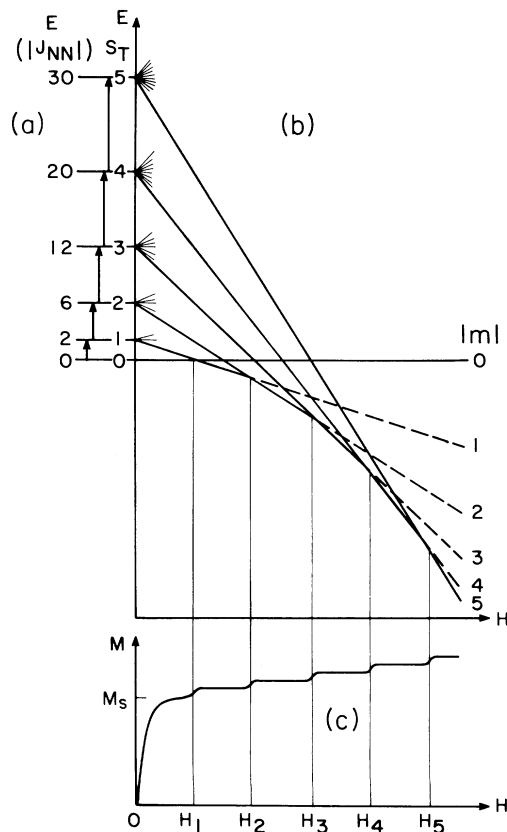


FIG. 2. (a) Energy-level diagram for a pair of NN Mn^{2+} ions at $H=0$. Adjacent levels are connected by arrows. (b) Zeeman splitting of these levels in a magnetic field H . (c) Schematic of the magnetization curve at low T , showing the plateau $M=M_s$, followed by magnetization steps due to the NN pairs.

$$E = -J_1[S_T(S_T+1) - 2S(S+1)] + g\mu_B mH, \quad (2)$$

where $S = \frac{5}{2}$ for an individual manganese ion.

The energy levels at $H=0$ are shown in Fig. 2(a). At this field they depend on S_T only. Figure 2(b) shows the Zeeman splitting of these levels. This splitting leads to many level crossings. Some of these crossings, at the fields H_1, H_2, \dots, H_5 , cause abrupt changes in the ground state of the pair. Each change of the ground state causes $|m|$ for the ground state to jump by one unit.

If the temperature T is low, $k_B T \ll 2|J_1|$, then the jump $|m|$ leads to a magnetization step. For NN consisting of Mn^{2+} ions, there are five such MST's. These are shown in Fig. 2(c). The MST's occur at fields

$$H_n = 2|J_1|n, \quad (3)$$

where $n = 1, 2, \dots, 5$. Equation (3) will be modified later, when more general models are considered.

Each of the five MST's gives rise to a peak in dM/dH vs H . In the NN cluster model this peak is symmetric, and its full width at half height, $(\delta H)_T$, is given by

$$g\mu_B(\delta H)_T = 3.53k_B T. \quad (4)$$

This "thermal width" is controlled only by the temperature. Other sources of broadening of the MST's will be considered later.

2. Dzyaloshinski-Moriya interaction

To go beyond the NN cluster model, additional interactions must be included. For a NN pair of Mn^{2+} ions the important additional interactions are the Dzyaloshinski-Moriya (DM) interaction,¹¹ and exchange interactions with distant neighbors. We consider the DM interaction first.

The two Mn ions comprising a NN pair are also coupled by a DM interaction,

$$\mathcal{H}_{DM} = -2\mathbf{D} \cdot \mathbf{S}_1 \times \mathbf{S}_2. \quad (5)$$

The direction of the vector \mathbf{D} is discussed later. The magnitude D of this vector is a measure of the strength of the DM interaction. For $\text{Cd}_{1-x}\text{Mn}_x\text{Se}$ the theoretical value obtained by Larson and Ehrenreich¹¹ is $|D/J_1| \cong 0.02$.

The effects of the DM interaction on the MST's were considered in Refs. 6, 8, and 12. Because $|D/J_1| \ll 1$, the DM interaction is treated as a perturbation. The starting point are the eigenstates $|S_T m\rangle$ of the Hamiltonian (1). Near each MST the two relevant states are mixed by the DM interaction. As a result of this mixing, the two energy levels no longer cross. Instead, they anticross. The calculated anticrossing near the first magnetization step in $\text{Cd}_{1-x}\text{Mn}_x\text{Se}$ is shown by the solid curves in Fig. 3(a). (The value of D used in this figure is reasonable, but is not exact.)

The anticrossing has no effect on the fields H_n at the centers of the MST's, i.e., they are still given by Eq. (3). However, it increases the widths of the MST's. To isolate this broadening mechanism, it is useful to consider the situation at $T=0$, where there is no thermal broadening.

The peak in dM/dH associated with n th step then has a full width at half height

$$g\mu_B(\delta H)_{DM} = 3.07|V_{DM}(n)|. \quad (6)$$

Here,

$$V_{DM}(n) \equiv \langle S_T' m' | \mathcal{H}_{DM} | S_T m \rangle$$

is the matrix element connecting the two states involved with the n th magnetization step at H_n . This matrix element depends on the step number n . Therefore, unlike the thermal width $(\delta H)_T$, the DM width $(\delta H)_{DM}$ depends on n . In addition to the dependence on n , $V_{DM}(n)$ is proportional to D_\perp , i.e., the component of \mathbf{D} perpendicular to \mathbf{H} . The calculated values of $V_{DM}(n)/D_\perp$ for all five steps, $n = 1, 2, \dots, 5$, are given in Table I. These were obtained using the Clebsch-Gordan coefficients¹³ for two spins with $S = \frac{5}{2}$. The matrix element for $n = 1$ was obtained earlier by McIntyre.¹² Note that the matrix element for $n = 2$ is approximately double that for $n = 1$. This means that the DM width for the second MST is roughly twice that for the first MST.

At a finite temperature the width of a magnetization step will be determined both by T and by $V_{DM}(n)$. Figure 3(b) shows computer-generated peaks of dM/dH near the first MST in $\text{Cd}_{1-x}\text{Mn}_x\text{Se}$. The dashed curve ignores the DM interaction, whereas the solid curve includes this interaction. Clearly the DM interaction broadens the dM/dH peak. The broadening implies a reduction in the peak's height, because the integral of the peak (which is the step size) is not affected by the DM interaction.

In the preceding discussion, and Fig. 3, all NN pairs in the sample were assigned the same matrix element $V_{DM}(n)$. This is equivalent to assuming the same D_\perp for all NN pairs. In reality the directions of the \mathbf{D} vectors for different pairs are different, so that D_\perp is not unique. Nevertheless, the main conclusions reached remain valid: The DM interaction leads to an anticrossing, it broadens the MST's, but it does not shift the fields H_n at which they occur.

3. Exchange interactions with distant neighbors

Besides the dominant exchange interaction with NN's there are also weaker exchange interactions with more distant neighbors. The effects of these distant-neighbor interactions on the MST's were discussed by Larson

TABLE I. The magnitude of the ratio $V_{DM}(n)/D_\perp$ for the five magnetization steps resulting from pairs of Mn^{2+} ions. $V_{DM}(n)$ is the matrix element for the DM interaction \mathcal{H}_{DM} in Eq. (5), between the two states involved in the n th MST. D_\perp is the component of \mathbf{D} perpendicular to \mathbf{H} .

n	$ V_{DM}(n)/D_\perp $
1	$(35/6)^{1/2} = 2.415$
2	$8(2/5)^{1/2} = 5.060$
3	$27/(14)^{1/2} = 7.216$
4	$(8/3)(10)^{1/2} = 8.433$
5	$5(5/2)^{1/2} = 7.906$

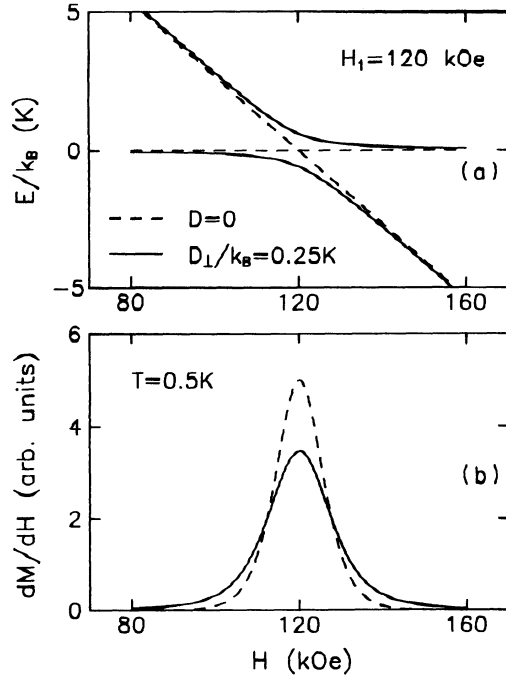


FIG. 3. (a) Calculated energy levels near the first magnetization step at H_1 . The dashed lines show the level crossing in the absence of the Dzyaloshinski-Moriya (DM) interaction. The solid lines show the anticrossing when the DM interaction is included. (b) Calculated differential susceptibility dM/dH near the first magnetization step. The dashed lines neglect the DM interaction. The solid lines include the broadening by the DM interaction. In these model calculations the broadening due to distant neighbors is ignored, and all NN's are assumed to be equivalent.

*et al.*¹⁴ The main conclusions are as follows.

First, the distant-neighbor interactions raise the fields H_n at the MST's. The fields H_n are then given by

$$g\mu_B H_n = 2|J_1|n + \Delta. \quad (7)$$

Equation (7) replaces Eq. (3). To a good approximation the "shift" Δ is independent of n . This result is important because it implies that J_1 can be obtained from the difference between two H_n 's, e.g.,

$$g\mu_B (H_2 - H_1) = 2|J_1|. \quad (8)$$

Second, the distant-neighbor interactions broaden the MST's. This broadening is asymmetric, in contrast with both the thermal broadening and the DM broadening, which are symmetric. The broadening due to distant neighbors increases with x , because there are more distant neighbors.

It follows that the broadening of the MST's is due to three separate sources: thermal, DM, and distant neighbors.

B. MST's for two inequivalent groups of NN's

1. Splitting of the MST's

The existence of in-plane and out-of-plane NN pairs in the wurtzite structure implies that there are two series of

MST's. They will occur at fields

$$g\mu_B H_n^{\text{in}} = 2|J_1^{\text{in}}|n + \Delta^{\text{in}}, \quad (9a)$$

and

$$g\mu_B H_n^{\text{out}} = 2|J_1^{\text{out}}|n + \Delta^{\text{out}}. \quad (9b)$$

The "shifts" Δ^{in} and Δ^{out} , which are due to distant-neighbor interactions, are not identical. The reason can be seen from the following example. Each Mn^{2+} ion in the wurtzite structure has two third-neighbor cations.¹⁴ These third neighbors are along the $\pm\hat{c}$ directions, at a distance $a(8/3)^{1/2}$. Therefore, there are four cations that are third neighbors of one or the other of the two members of a NN pair. For an in-plane NN pair ("IN pair") any of the four third-neighbor positions may be occupied by Mn^{2+} . But in the case of an out-of-plane NN pair ("OUT pair"), only two of the four third-neighbor positions may be occupied by Mn^{2+} . The other two positions cannot be occupied because besides being third-neighbor positions for one member of the pair they are also nearest-neighbor positions for the other member. Had these positions been occupied by Mn^{2+} , the NN pair would have become a NN triplet or a larger NN cluster. The difference between the number of third-neighbor positions available for occupation implies that the average effective field due to third neighbors is larger for IN pairs than for OUT pairs.

To calculate the overall difference between Δ^{in} and Δ^{out} one has to consider all possible distant neighbors. This has not been done yet. Nevertheless, we expect the difference $\Delta^{\text{in}} - \Delta^{\text{out}}$ to be small compared to either Δ . One reason is that the number of NNN positions that can be occupied by Mn^{2+} is the same for both groups of NN pairs. This fact is significant because among the distant-neighbor interactions, the interaction with the NNN's is expected to be the largest.⁵

When the difference ΔJ_1 is small compared to \bar{J}_1 , the "in" and "out" series of MST's given by Eqs. (9) will be close to each other. In that case when the two series are completely resolved they will have the appearance of a single series of MST's in which each MST is split into a doublet of smaller steps. These two smaller steps will have equal heights because there are equal numbers of IN and OUT NN's. Thus the height of each of the two smaller steps is one half of the total height of the MST. For this reason the two smaller steps in a doublet will be called "half-steps."

Ignoring the small difference between Δ^{in} and Δ^{out} in Eqs. (9), the separation $|H_n^{\text{in}} - H_n^{\text{out}}|$ between the two half-steps associated with the n th MST is proportional to n . The optimal conditions for resolving the two half-steps are therefore the lowest possible T and x (to reduce the width), and the highest possible H (to increase the splitting, which is proportional to n).

Equations (9a) and (9b) indicate that the fields at the half-steps are determined both by the J_1 's and by the Δ 's. We expect that in the great majority of materials the difference between Δ^{in} and Δ^{out} will be small compared with ΔJ_1 . In that case, the half-step associated with the smaller $|J_1|$ will always occur at the lower field. Analysis

of the present data shows that this is the case for the samples used in the present experiments.

2. Obtaining \bar{J}_1 and $|\Delta J_1|$

If more than one doublet is resolved, and if, in addition, one knows which half-step is the IN half-step and which is the OUT half-step then both J_1^{in} and J_1^{out} can be obtained easily. That is, from Eqs. (9a) and (9b),

$$g\mu_B(H_2^{\text{in}} - H_1^{\text{in}}) = 2|J_1^{\text{in}}|, \quad (10a)$$

and

$$g\mu_B(H_2^{\text{out}} - H_1^{\text{out}}) = 2|J_1^{\text{out}}|. \quad (10b)$$

The main difficulty in carrying out this procedure is that even when the doublets are resolved, it is not immediately obvious whether the upper or the lower half-step in a doublet is the IN half-step. In the absence of this information, one can determine $\bar{J}_1 \equiv \frac{1}{2}(J_1^{\text{in}} + J_1^{\text{out}})$ and $|\Delta J_1| = |J_1^{\text{in}} - J_1^{\text{out}}|$, but not the sign of ΔJ_1 .

Let the two half-steps associated with the first MST be at H_1' and H_1'' , and let those associated with the second MST be at H_2' and H_2'' . We choose $H_1'' > H_1'$, and $H_2'' > H_2'$. Define the average values

$$\bar{H}_1 = \frac{1}{2}(H_1' + H_1''), \quad \bar{H}_2 = \frac{1}{2}(H_2' + H_2''), \quad (11)$$

and the differences

$$\Delta H_1 = H_1'' - H_1', \quad \Delta H_2 = H_2'' - H_2'. \quad (12)$$

Then from Eqs. (10)

$$g\mu_B(\bar{H}_2 - \bar{H}_1) = 2|\bar{J}_1| \quad (13)$$

and

$$g\mu_B(\Delta H_2 - \Delta H_1) = 2|\Delta J_1|. \quad (14)$$

In some cases, two MST's are observed but at least one of the doublets is not resolved. The average value, \bar{H}_n , for any unresolved doublet can still be obtained from the data quite accurately, although not ΔH_n . The average exchange constant \bar{J}_1 is then calculated from Eq. (13). The average shift $\bar{\Delta} = \frac{1}{2}(\Delta^{\text{in}} + \Delta^{\text{out}})$ in Eqs. (9) can also be obtained, i.e.,

$$\bar{\Delta} = g\mu_B(2\bar{H}_1 - \bar{H}_2). \quad (15)$$

If only one of the doublets is resolved then an approximate value for $|\Delta J_1|$ can be obtained by ignoring the difference between Δ^{in} and Δ^{out} in Eqs. (9). This gives

$$g\mu_B \Delta H_1 \cong 2|\Delta J_1| \quad (16a)$$

and

$$g\mu_B \Delta H_2 \cong 4|\Delta J_1|. \quad (16b)$$

The precision of Eqs. (16) will be discussed in connection with the data analysis.

3. Obtaining the sign of $\Delta J_1 / \bar{J}_1$

To determine which NN exchange constant, J_1^{in} or J_1^{out} , is the larger it is necessary to find out which member of an observed doublet is due to the IN pairs and which to the OUT pairs. Such an identification can be made on the basis of the difference in the widths of the two half-steps. The method is based on the following facts: (1) The width of each half-step is governed, in part, by the DM interaction. (2) The matrix element $V_{\text{DM}}(n)$, which controls the DM width, is proportional to D_{\perp} . (3) For a given direction of \mathbf{H} , D_{\perp} depends on the direction of the \mathbf{D} vector. (4) The direction of \mathbf{D} depends on the orientation of the NN pair relative to the crystal axes. It follows that there is a correlation between the spatial orientation of the NN pair and the contribution of this NN to the width of the half-step. This is the key to the identification of the half-steps.

The magnitude of D_{\perp} is governed by two factors: the magnitude D of the \mathbf{D} vector, and its orientation relative to \mathbf{H} . To simplify the discussion we assume that the magnitude of \mathbf{D} is the same for IN and OUT pairs, i.e., $D^{\text{in}} = D^{\text{out}} = D$. The rationale for this assumption is that a small difference between the D 's (comparable to the observed 15% difference between the J_1 's) has little effect on the discussion. The possibility of a large difference between D^{in} and D^{out} is addressed later.

In the zinc-blende structure the \mathbf{D} vector for a given NN pair is perpendicular to the triad consisting of the two magnetic ions in the pair and the unique intervening anion.¹¹ This is also expected to be true for the wurtzite structure.⁹ Using the geometry of Fig. 1 one can then show that the \mathbf{D} vector for any OUT pair is perpendicular to the c axis. (The \mathbf{D} vectors of the various OUT pairs are along different directions in the c plane. These directions are related by symmetry.) On the other hand, the \mathbf{D} vectors for all IN pairs in the ideal wurtzite structure make an angle $\alpha = \sin^{-1}[(1/3)^{1/2}] = 35.3^\circ$ with the c axis.

When \mathbf{H} is parallel to the c axis, $D_{\perp} = D$ for all OUT pairs, whereas $D_{\perp} = D/\sqrt{3}$ for all IN pairs. The IN half-step is then narrower. Therefore, the dM/dH peak associated with the IN half-step is taller and narrower than the OUT peak. Of course, these differences will be appreciable only if the DM broadening is a major source of the overall broadening.

Figure 4 shows computer simulations of the dM/dH doublet arising from the splitting of a MST in the wurtzite structure. The field \mathbf{H} is parallel to the c axis. The parameters are roughly, but not exactly, those for the second MST in $\text{Cd}_{1-x}\text{Mn}_x\text{Se}$. For these simulations we chose $|J_1^{\text{in}}| > |J_1^{\text{out}}|$ so that the IN member of the doublet is at the higher field.

The preceding discussion indicates that in experiments with $\mathbf{H} \parallel \hat{c}$, that member of the doublet which has a narrower and taller dM/dH peak is the IN member. One possible objection to this identification is that a difference in widths can also arise from a large difference between D^{in} and D^{out} , or from a large difference between the distant-neighbor widths. Such possibilities are remote, in our view. Fortunately, they can also be ruled out by a

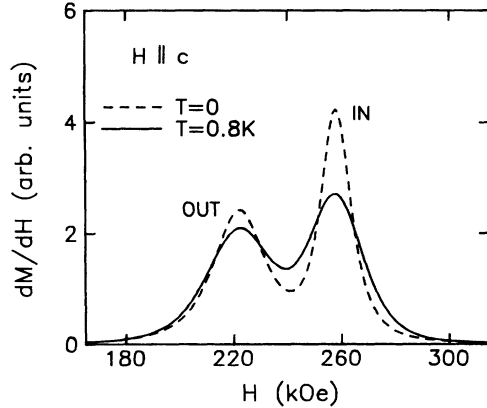


FIG. 4. Calculated line shape of dM/dH near the second MST, showing the doublet resulting from inequivalent NN's in the wurtzite structure. The magnetic field \mathbf{H} is parallel to the c axis. The parameters in these simulations are roughly, but not exactly, equal to those for $\text{Cd}_{1-x}\text{Mn}_x\text{Se}$, namely, $\bar{H}_2 = 240$ kOe, $|\Delta J_1/\bar{J}_1| = 0.15$, $|J_1^{\text{in}}| > |J_1^{\text{out}}|$, $D/k_B = 0.20$ K. Distant-neighbor broadening is ignored. The dashed curve is for $T=0$, whereas the solid curve is for $T=0.8$ K. Note that the IN peak is taller and narrower than the OUT peak.

control experiment in which \mathbf{H} is in the c plane.

When \mathbf{H} is in the c plane the value of D_{\perp} is not the same for all IN pairs, or for all OUT pairs. The IN half-step is then a superposition of smaller steps, all at the same field H_n^{in} but with different widths due to the different D_{\perp} . The same is true for the OUT half-step. The overall width of either the IN or the OUT half-step can be shown to depend on the orientation of \mathbf{H} in the c plane. This dependence is much stronger for the OUT half-step. Despite this dependence, some general statements can be made for any field direction in the c plane.

(1) If D is approximately the same for the IN and OUT groups then the dM/dH peak associated with the OUT half-step is always narrower and taller than the IN peak. This is just the opposite to the situation when \mathbf{H} is parallel to the c axis.

(2) When the direction of \mathbf{H} changes from the c axis to any direction in the c plane, the dM/dH peak associated with the IN half-step widens and its maximum decreases. At the same time the OUT peak narrows and becomes taller.

The statements in (2) can be proved easily. Statement (1) is based on computer simulations. The fact that the difference between the IN and OUT line widths changes sign on going from $\mathbf{H}||\hat{c}$ to $\mathbf{H}\perp\hat{c}$ provides a powerful check on the identification of the half-steps.

4. Estimating D

Upper and lower limits for D , as well as a rough estimate for D can be obtained readily from the line shape of a doublet.

A very conservative upper limit for D is obtained by assuming that the width of each member of a resolved doublet is entirely due to the DM interaction. The procedure is simplest when \mathbf{H} is parallel to the c axis. Using

Eq. (6) and the observed width, an upper limit for $V_{\text{DM}}(n)$ is obtained. Table I is then used to obtain an upper limit for D_{\perp} . For $\mathbf{H}||\hat{c}$, $D_{\perp} = D$ for the OUT group, and $D_{\perp} = D/\sqrt{3}$ for the IN group. Thus, the upper limit for D_{\perp} yields an upper limit for D . A less conservative upper limit is obtained by ascribing the width to *both* the DM interaction and the temperature (but still ignoring the distant neighbors). This procedure requires computer simulations in which T is fixed, at the actual temperature, and D is varied until the observed width is matched.

A lower limit for D can be obtained when the two members of a doublet for $\mathbf{H}||\hat{c}$ have different widths, and when the DM origin of this difference is confirmed by a control experiment with $\mathbf{H}\perp\hat{c}$. One procedure uses computer simulations in which T is held fixed at the measurement temperature. The value of D is then increased until the observed percentage difference in the widths is obtained. This is a lower limit for D because distant-neighbors broadening is ignored; for given T and D the distant neighbors should reduce the percentage difference between the widths. Sometimes it is more practical to focus on the difference between the *heights* of the dM/dH peaks rather than on the difference in the widths.

A rough estimate for D can be obtained by assuming that: (1) distant-neighbor broadening is the same for both the IN and OUT half-steps, and (2) this broadening can be represented as an increase in the effective temperature. Fixing D , the effective temperature T_{eff} is adjusted until the width of one member of the doublet is reproduced. The width of the other member is then fully determined, since both D and T_{eff} are fixed. A correct initial choice for D will reproduce the width of the second member. The procedure is carried out using computer simulations for various initial choices of D , until the correct choice is found. This method of finding D is only approximate because the two assumptions on which it is predicated (concerning distant-neighbor broadening) are not rigorously correct.

III. EXPERIMENTAL TECHNIQUES

Two Bridgman-grown single crystals of $\text{Cd}_{1-x}\text{Mn}_x\text{Se}$ were used. Their nominal compositions were $x = 1.0$ and 2.5% . These values were confirmed by high-field magnetization measurements. (The magnetization M_s at the plateau in Fig. 1 is related to x , as discussed in Refs. 6 and 15.) Microprobe measurements on the sample with $x(\text{nominal}) = 2.5\%$ gave $x = 2.35\%$. The microprobe analysis of this sample also showed that x was quite uniform, i.e., $|(x - \bar{x})/\bar{x}| < 0.05$ for all the "spots" scanned. The direction of the c axis in the sample with $x = 2.5\%$ was found using x-rays. The sample with $x = 1\%$ was not oriented.

Magnetization measurements were carried out using two types of magnets: hybrid magnets with maximum fields of 27 and 30 T, and several 20 T Bitter magnets. The experiments were performed either at 0.5–0.6 K using ^3He , or at ~ 80 mK using a dilution refrigerator. Data in ^3He were obtained in all the magnets, but the data in the dilution refrigerator were taken only in one of the 20 T Bitter magnets.

The magnetization was measured with two magnetometers: A vibrating sample magnetometer (VSM), modified for use in high-field magnets, was used to take the data in ^3He . A force magnetometer was used in the dilution refrigerator at ~ 80 mK. The design of the force magnetometer has been described previously by Swanson *et al.*¹⁶

To improve the signal-to-noise ratio, several traces of the magnetization M vs H were taken for each experimental configuration. The results of all the traces were then averaged using a computer. Individual traces were also analyzed, to evaluate the consistency of the traces.

IV. RESULTS AND DISCUSSION

A. General features

The MST's in $\text{Cd}_{1-x}\text{Mn}_x\text{Se}$ have been studied previously.^{10,15,17,18} The focus of the present experiments is on the splitting of the MST's due to the two inequivalent groups of NN's.

The first two MST's ($n=1,2$) were observed both in the sample with $x=1.0\%$ and in the sample with $x=2.5\%$. A panoramic view of the two MST's is shown in Fig. 5(a). The derivative dM/dH of this trace, obtained by a numerical differentiation, is shown in Fig. 5(b). These data, which are for $x=2.5\%$, were obtained

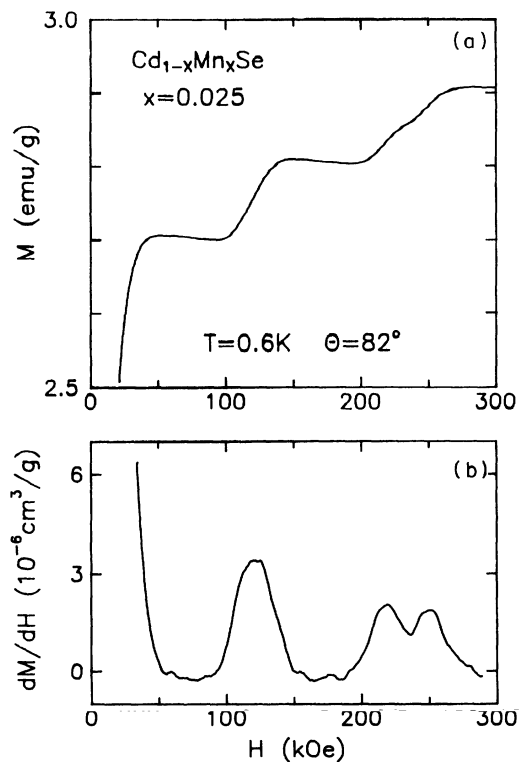


FIG. 5. (a) Measured high-field magnetization of $\text{Cd}_{0.975}\text{Mn}_{0.025}\text{Se}$ at 0.6 K, showing the first two magnetization steps. The second MST is split into two half-steps. These data were taken with the field H at an angle $\theta=82^\circ$ from the c axis. (b) The differential susceptibility dM/dH obtained by a numerical differentiation of the data in part (a).

in the 30 T hybrid magnet at 0.6 K. Note that the second MST is split into two half-steps, whereas the splitting of the first MST is not resolved at this temperature. Figure 6(a) shows the first MST in the sample with $x=1.0\%$, measured at 0.5 K. The derivative, dM/dH , is shown in Fig. 6(b). There is no clear splitting of the first MST in this case either, even though the distant-neighbor broadening for $x=1.0\%$ is smaller than for $x=2.5\%$ and the temperature is slightly lower than in Fig. 5. Only in the dilution refrigerator did the splitting of the first MST become clearly resolved, both for $x=1.0\%$ and 2.5% . The data in this refrigerator were taken at 0.08 K. Figure 7 shows an example of the results for $x=2.5\%$.

In Fig. 6(a) the measured magnetization curve (solid line) has a negative slope both before and after the MST. This negative slope is due to the diamagnetic susceptibility of the lattice, $\chi_d = -3.3 \times 10^{-7}$ emu/g. The dashed line in Fig. 6(a) shows the same data, but after a correction for the diamagnetism of the lattice. The magnetization data for $x=2.5\%$ [Fig. 5(a)] also show the negative slope due to χ_d , before and after the first MST. For this higher x , however, the lattice diamagnetism is relatively less important because the signal from the manganese ions is stronger.

Figures 5 and 6 show that the size of the MST's is much larger for $x=2.5\%$ than for $x=1\%$. The reasons are a larger Mn concentration, and a higher probability

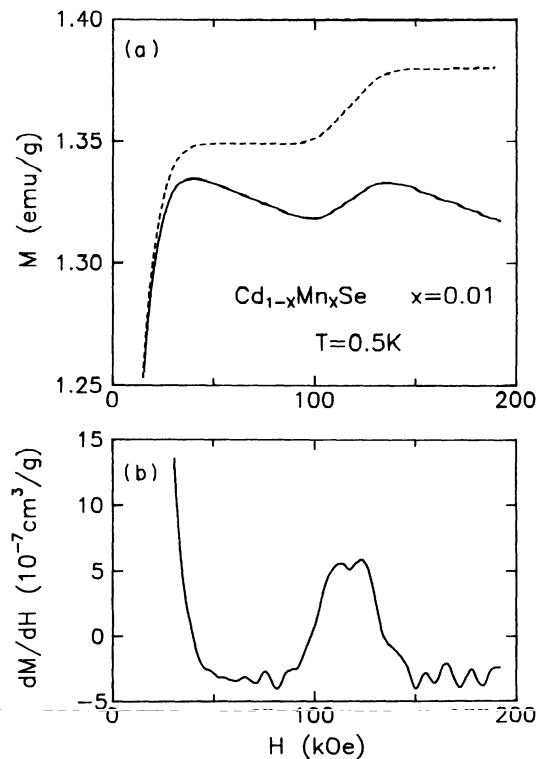


FIG. 6. (a) The solid curve shows the magnetization of $\text{Cd}_{0.99}\text{Mn}_{0.01}\text{Se}$ near the first MST, measured at 0.5 K. The dashed curve shows the same data after a correction for the diamagnetism of the lattice. (b) The differential susceptibility dM/dH obtained by a numerical differentiation of the solid curve in part (a).

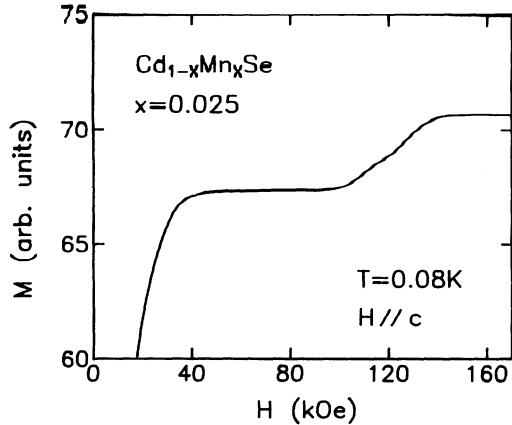


FIG. 7. Measured magnetization of $\text{Cd}_{0.975}\text{Mn}_{0.025}\text{Se}$ at 0.08 K, showing the splitting of the first MST into two half-steps. These data are for \mathbf{H} parallel to the c axis.

that a Mn ion is in a NN pair. The larger signal for $x=2.5\%$ resulted in higher-quality data as compared to $x=1.0\%$. For this reason the most extensive data were taken on the sample with $x=2.5\%$. This is the only sample in which the dependence of the splitting on the angle θ between \mathbf{H} and the c axis was measured. Two early experimental runs on this sample were taken at an angle θ which was later determined to be 82° . Both of these runs were in hybrid magnets (see the example in Fig. 5). Because an angle of 82° is reasonably close to 90° , it was decided not to repeat these experiments at exactly 90° . All the later experiments on the same sample were either at $\theta=0$ ($\mathbf{H}||\hat{c}$) or at $\theta=90^\circ$ ($\mathbf{H}\perp\hat{c}$). The sample with $x=1.0\%$ was not oriented, and the angle θ could not be determined after the experiments were completed.

B. Determining \bar{J}_1 and $|\Delta J_1|$

The values of \bar{J}_1 and $|\Delta J_1|$ were obtained from H'_n and H''_n ($n=1,2$) using equations given in Sec. II B 2. The values of H'_n and H''_n at the centers of the two half-steps associated with n th MST were obtained using two alternative procedures: One focused on the derivative dM/dH vs H , while the other focused on the magnetization curves M vs H . The measured derivative dM/dH was fitted to the sum of two Gaussians having equal integrals. [The integral $\int (dM/dH)dH$ of each Gaussian is the size of the half-step.] In addition to H'_n and H''_n , the widths of the two Gaussians, and the common value of their integrals were treated as adjustable parameters. In the second procedure, each MST was regarded as a sum of two thermally broadened half-steps having equal heights. A fit of the curve for M vs H was then made with the following adjustable parameters: H'_n and H''_n , two effective broadening temperatures, and a common height for both half-steps. The two procedures led to very similar (although not identical) results. The results for H'_n , or H''_n , were then averaged. The estimated uncertainties in these fields were based in part on the differences between the results of the two procedures.

The value of $\bar{J}_1 \equiv \frac{1}{2}(J_1^{\text{in}} + J_1^{\text{out}})$ was determined from \bar{H}_1 and \bar{H}_2 using Eq. (13) and letting $g=2.00$ for the g factor of the Mn^{2+} ion.¹⁹ For $x=2.5\%$ the results of three runs in which both the first and the second MST's were observed gave: $\bar{J}_1/k_B = -7.65 \pm 0.1$, -7.50 ± 0.1 , and -7.58 ± 0.1 K. For $x=1.0\%$, only a single run was performed in fields sufficiently high to observe the second MST. This run gave $\bar{J}_1/k_B = -7.48 \pm 0.1$ K. Using the average of these values we conclude that $\bar{J}_1/k_B = -7.55 \pm 0.1$ K. This result is in excellent agreement with recent values obtained by our group.^{10,18}

Approximate values for $|\Delta J_1| \equiv |J_1^{\text{in}} - J_1^{\text{out}}|$ were obtained from the splitting ΔH_n of a single MST, using Eqs. (16). In addition, Eq. (14) which relates $|\Delta J_1|$ to the splittings of *both* MST's was also used. Although the latter equation is exact, it does not necessarily yield more accurate results because it involves the experimental uncertainties in both splittings.

For $x=2.5\%$ the splitting ΔH_2 of the second MST gave $|\Delta J_1|/k_B = 1.13 \pm 0.03$ K (based on three experimental runs, in each of which several traces of the second MST were taken). For $x=1.0\%$, ΔH_2 gave 1.17 ± 0.07 K (from a single run). The splitting ΔH_1 of the first MST gave 1.21 ± 0.1 K for the sample with $x=2.5\%$ (three runs), and 1.12 ± 0.07 K for $x=1.0\%$ (a single run). These results assume that Eqs. (16) are exact, which is not the case because the derivation of Eqs. (16) neglects the difference between Δ^{in} and Δ^{out} in Eqs. (9). To estimate the error that resulted from the use of Eqs. (16) we assumed that the difference between the two Δ 's was less than 20% of their average $\bar{\Delta}$. Equation (15) was used to obtain $\bar{\Delta}$. On this basis the error in the value of $|\Delta J_1|$ obtained from ΔH_2 is less than 5% for $x=2.5\%$, and less than 3% for $x=1.0\%$. The maximum possible errors for the values obtained from the splitting ΔH_1 of the first MST are twice as large.

Using the splittings of *both* MST's and Eq. (14) we obtained $|\Delta J_1|/k_B = 1.06 \pm 0.12$ K for $x=2.5\%$, and 1.21 ± 0.15 K for $x=1.0\%$. Based on all the results, obtained using both Eqs. (16) and Eq. (14), we conclude that $|\Delta J_1|/k_B = 1.15 \pm 0.08$ K. The corresponding value of $|\Delta J_1/\bar{J}_1|$ is 0.15 ± 0.01 . This final result for $|\Delta J_1/\bar{J}_1|$ is close to the value 0.13 obtained experimentally for $\text{Cd}_{1-x}\text{Mn}_x\text{S}$ (Ref. 8), and is also in good agreement with the theoretical estimate 0.16 obtained by Larson.⁹

C. Determining which NN exchange constant is the larger

To determine which NN exchange constant, J_1^{in} or J_1^{out} , is the larger, it is necessary to know which of the two half-steps at H'_n and H''_n is the IN half-step. Such an identification was made on the basis of the relative heights of the two peaks in dM/dH . As discussed in Sec. II B 3, for $\mathbf{H}||\hat{c}$ the dM/dH peak associated with the IN pairs should be taller and narrower than the OUT peak. For $\mathbf{H}\perp\hat{c}$, one the other hand, the OUT peak should be taller and narrower than the IN peak.

Figure 8(a) shows dM/dH near the first MST for the configuration $\mathbf{H}||\hat{c}$. These results were obtained by a numerical differentiation of the curve in Fig. 7. Clearly, the

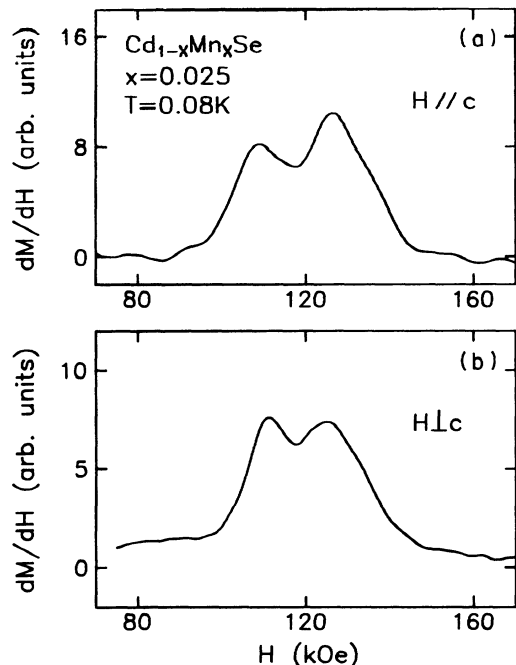


FIG. 8. Differential susceptibility of $\text{Cd}_{0.975}\text{Mn}_{0.025}\text{Se}$ near the first MST at 0.08 K. (a) Results for \mathbf{H} parallel to the c axis. (b) Results for \mathbf{H} perpendicular to the c axis. These results were obtained by a numerical differentiation of the corresponding magnetization curves. The ordinate scales for parts (a) and (b) are different.

peak associated with the half-step which is at the higher field, H'_1 , is the taller of the two peaks. Similar results were obtained when this experiment was repeated using another force magnetometer, i.e., the half-step that is at the higher field gave a significantly taller peak in the derivative dM/dH . On this basis the half-step at the higher field is the IN half-step, so that J_1^{in} is larger in magnitude than J_1^{out} .

To verify this conclusion it is necessary to rule out other possible mechanisms that can cause the peak at H'_1 to be taller when \mathbf{H} is parallel to \hat{c} . One such mechanism is a difference between the distant-neighbor broadening of the two half-steps. (The peak in dM/dH for a broader half-step is necessarily smaller in height.) One characteristic of this mechanism is that it is independent of the orientation of \mathbf{H} . But the data for $\mathbf{H} \perp \hat{c}$ in Fig. 8(b) show that the peak at H'_1 is taller than that at H'_2 . This is just the opposite to the result for $\mathbf{H} \parallel \hat{c}$. Thus, a difference between the distant-neighbor broadening of the two half-steps cannot explain the data.

A second mechanism that could cause the height difference in Fig. 8(a) is an asymmetry in each individual peak, due to the asymmetric broadening by the distant neighbors. If the asymmetry is such that the "tail" on the high-field side is larger, then the peak at H'_1 would be superimposed on a larger tail. This would cause the peak at H'_1 to appear taller. However, since this mechanism too is independent of the orientation of \mathbf{H} , it cannot account for the difference between the results for $\mathbf{H} \parallel \hat{c}$ and $\mathbf{H} \perp \hat{c}$.

Finally, suppose that it is actually the peak in H'_1 which is the IN peak, and that the reason that this peak is smaller, for $\mathbf{H} \parallel \hat{c}$, is that D^{in} is larger than D^{out} by more than a factor of $\sqrt{3}$. If this were the case then when \mathbf{H} was rotated from parallel to perpendicular to \hat{c} , the peak at H'_1 would have become even smaller in relation to the peak at H'_2 . Because Figs. 8(a) and 8(b) show the opposite behavior, the peak at H'_1 must be the OUT peak. It follows that J_1^{out} is smaller in magnitude than J_1^{in} .

The same conclusion is reached on the basis of the second MST. The dM/dH results for this MST, both for $\mathbf{H} \parallel \hat{c}$ ($\theta=0$) and for $\theta=82^\circ$, are shown in Fig. 9. Both sets of data were obtained in 27 T hybrid magnets. The crucial result for $\theta=0$ is that the peak at the higher field, H'_2 , is the taller of the two peaks. For $\theta=82^\circ$, the opposite is true. This indicates, again, that the magnitude of J_1^{in} is larger than that of J_1^{out} . This result agrees with Larson's prediction.

Two features of Fig. 9 require some comment: (1) The limited field range for $\theta=0$ is due to the fact that only the second MST was studied in this experimental run. (2) The data for $\theta=82^\circ$ are similar to those in Fig. 5(b), ex-

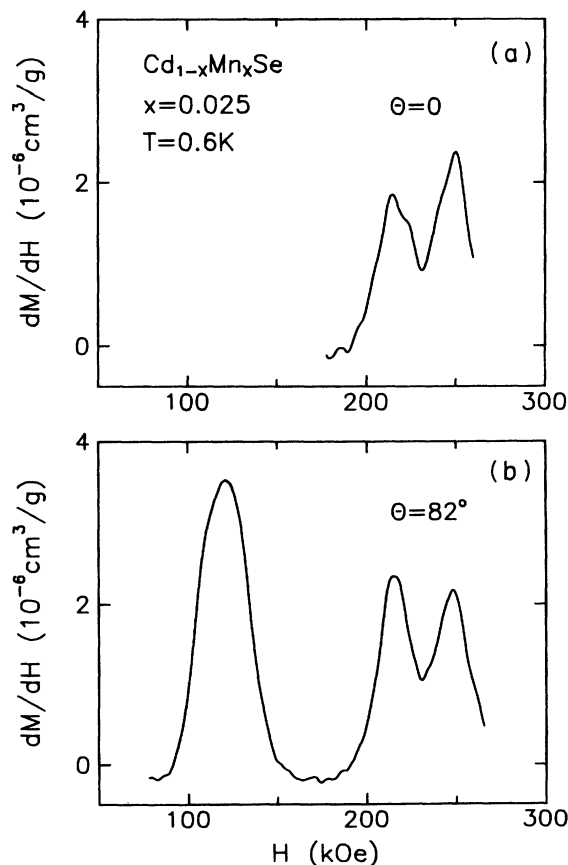


FIG. 9. Differential susceptibility dM/dH of $\text{Cd}_{0.975}\text{Mn}_{0.025}\text{Se}$ at 0.6 K. (a) Results near the second MST for $\theta=0$, i.e., \mathbf{H} parallel to the c axis. (b) Results near the first and second MST's when \mathbf{H} makes an angle of 82° with the c axis. These results were obtained by numerical differentiation of the corresponding magnetization curves.

cept that they have a higher signal-to-noise ratio and they do not extend beyond 27 T. The similarity to the results in Fig. 5(b) attests to the reproducibility of the data.

D. Estimate for D

An upper limit for the DM interaction constant D was obtained from the widths of the half-steps. It was assumed that the width was due to both DM broadening and thermal broadening at the operating temperature. Because distant neighbors were ignored, this is an upper limit for D (see Sec. II B 4).

The half-steps of the second MST were the most useful because the upper limits deduced from them were substantially smaller than those deduced from the half-steps of the first MST. The likely reason for this is that the ratio between the broadening due to distant neighbors and the DM broadening is smaller for the second MST, because of the larger matrix element $V_{\text{DM}}(n)$. From the width of the OUT half-step at H'_2 an upper limit of about 0.24 K for D/k_B was obtained. The IN half-step at H''_2 gave an upper limit of about 0.30 K. The likely reason why the IN upper limit is higher than the OUT upper limit is that the DM broadening was smaller for the IN half-step so that the neglected distant-neighbor broadening was relatively more important. The most useful upper limit is the smallest, i.e., $D/k_B < 0.24$ K.

A lower limit for D was obtained from the difference between the heights of the two half-steps in the configuration $\mathbf{H} \parallel \hat{\mathbf{c}}$ (see Sec. II B 4). The half-steps comprising the second MST were used. Computer simulations were made in which T was kept fixed at the experimental value, 0.6 K, and D was increased gradually. For $D/k_B = 0.06$ K, the calculated difference in the heights of the two dM/dH peaks is 5%, which is far too small. The value of D/k_B that reproduces the observed difference in heights is about 0.14 K. To be on the conservative side, we chose $D/k_B = 0.10$ K as the lower limit. This D gives a height difference of 14%, which is somewhat above half of the observed difference. The half-steps of the first MST, measured at 0.08 K, give a smaller lower limit for D , which is less useful. Combining the upper and lower limits, $0.10 < D/k_B < 0.24$ K.

Estimates for D were obtained from the line shapes of

the doublets associated with the first and second MST's. The data for $\mathbf{H} \parallel \hat{\mathbf{c}}$ were used for this purpose. The procedure matched the widths of the two half-steps in a given doublet using a common D and a common effective broadening temperature T_{eff} (see Sec. II B 4). From the doublet associated with the second MST an estimate $D/k_B \cong 0.21$ K was obtained. The doublet associated with the first MST gave $D/k_B \cong 0.27$ K. These estimates for D assume that $D^{\text{in}} = D^{\text{out}} = D$. If one assumes instead that D is proportional to J_1 (i.e., the difference $D^{\text{in}} - D^{\text{out}}$ is equal to 15% of the average value \bar{D}) then the estimated values of \bar{D} are $\sim 15\%$ higher than those quoted above.

The estimate $D/k_B = 0.27$ K deduced from the line shape of the first MST is higher than the upper limit 0.24 K obtained earlier. This discrepancy does not constitute a contradiction, however, because (1) the upper limit was obtained from the second MST, not from the first, and (2) the value 0.27 K is only an estimate based on simplifying assumptions for distant-neighbor broadening. Our belief is that the estimate 0.21 K obtained from the second MST is more reliable because the ratio between the DM broadening and the distant-neighbor broadening is larger in this case, so that the result is less sensitive to the simplifying assumptions concerning distant-neighbor broadening.

Summarizing the results for D , the upper and lower limits give $0.10 < D/k_B < 0.24$ K. The best estimate based on the present experiments is $D/k_B \cong 0.21$ K. These results should be compared with the value $D/k_B = 0.16$ K calculated theoretically by Larson and Ehrenreich.¹¹

ACKNOWLEDGMENTS

We are grateful to S. Foner and D. Heiman for useful discussions. The work at Tufts University was supported by NSF Grant No. DMR-8900419. Partial support for the work at Brown University was received from the Office of Naval Research. The Francis Bitter National Magnet Laboratory is supported by NSF Cooperative Agreement DMR-8813164. V.B. was supported by the University of São Paulo, and C.C.A. was supported by IBM.

*Permanent address: Instituto de Física, Universidade de São Paulo, Caixa Postale 20516, CEP 05198, São Paulo, SP, Brazil.

¹*Diluted Magnetic (Semimagnetic) Semiconductors*, MRS Symposia Proceedings, Vol. 89, edited by R. L. Aggarwal, J. K. Furdyna, and S. von Molnar (MRS, Pittsburgh, 1987).

²*Diluted Magnetic Semiconductors*, Vol. 25 of *Semiconductors and Semimetals*, edited by J. K. Furdyna and J. Kossut (Academic, Boston, 1988).

³*Semimagnetic Semiconductors and Diluted Magnetic Semiconductors*, edited by M. Averous and M. Balkanski (Plenum, London, 1991).

⁴J. K. Furdyna, *J. Appl. Phys.* **64**, R29 (1988).

⁵B. E. Larson, K. C. Hass, H. Ehrenreich, and A. E. Carlsson, *Phys. Rev. B* **37**, 4137 (1988); B. E. Larson and H. Ehrenreich, *J. Appl. Phys.* **67**, 5084 (1990).

⁶Y. Shapira, *J. Appl. Phys.* **67**, 5090 (1990), and in Ref. 3.

⁷D. U. Bartholomew, E.-K. Suh, S. Rodriguez, A. K. Ramdas, and R. L. Aggarwal, *Solid State Commun.* **62**, 235 (1987).

⁸Y. Shapira, S. Foner, D. Heiman, P. A. Wolff, and C. R. McIntyre, *Solid State Commun.* **71**, 355 (1989).

⁹B. E. Larson, *J. Appl. Phys.* **67**, 5240 (1990).

¹⁰Early indications of the splitting of the MST's in $\text{Cd}_{1-x}\text{Mn}_x\text{Se}$ came from pulsed-field work by our group. Measurements of dM/dH [S. Foner *et al.*, *Phys. Rev. B* **39**, 11 793 (1989); and (unpublished)] and of the Faraday rotation [D. Heiman *et al.*

- (unpublished)] showed a wide, but unresolved, second MST and an apparently resolved third MST. Later unpublished dM/dH measurements in pulsed fields, by S. Foner, showed a splitting of the first MST. A wide, but unresolved, Raman line observed in Ref. 7 was also an early indication of a possible splitting.
- ¹¹B. E. Larson and H. Ehrenreich, *Phys. Rev. B* **39**, 1747 (1989).
- ¹²C. R. McIntyre, Ph.D. thesis, Physics Department, MIT, 1990.
- ¹³J. Owen and E. A. Harris, in *Electron Paramagnetic Resonance*, edited by S. Geschwind (Plenum, New York, 1972).
- ¹⁴B. E. Larson, K. C. Hass, and R. L. Aggarwal, *Phys. Rev. B* **33**, 1789 (1986).
- ¹⁵Y. Shapira, S. Foner, D. H. Ridgley, K. Dwight, and A. Wold, *Phys. Rev. B* **30**, 4021 (1984).
- ¹⁶A. G. Swanson, Y. P. Ma, J. S. Brooks, R. M. Markiewicz, and N. Miura, *Rev. Sci. Instrum.* **61**, 848 (1990).
- ¹⁷R. L. Aggarwal, S. N. Jasperson, Y. Shapira, S. Foner, T. Sakakibara, T. Goto, N. Miura, K. Dwight, and A. Wold, in *Proceedings of the 17th International Conference on the Physics of Semiconductors, San Francisco, 1984*, edited by J. D. Chadi and W. A. Harrison (Springer, New York, 1985), p. 1419.
- ¹⁸E. D. Isaacs, D. Heiman, P. Becla, Y. Shapira, R. Kershaw, K. Dwight, and A. Wold, *Phys. Rev. B* **38**, 8412 (1988).
- ¹⁹R. S. Title, *Phys. Rev.* **130**, 17 (1963).